

# The Elements of the Neutrino Mass Matrix: Allowed Ranges and Implications of Texture Zeros

Alexander Merle<sup>\*</sup>, Werner Rodejohann<sup>†</sup>

*Physik-Department, Technische Universität München,  
James-Frank-Strasse, D-85748 Garching, Germany*

## Abstract

We study the range of the elements of the neutrino mass matrix  $m_\nu$  in the charged lepton basis. Neutrino-less double beta decay is sensitive to the  $ee$  element of  $m_\nu$ . We then analyze the phenomenological implications of single texture zeros. In particular, interesting predictions for the effective mass can be obtained, in the sense that typically only little cancellation due to the Majorana phases is expected. Some cases imply constraints on the atmospheric neutrino mixing angle.

---

<sup>\*</sup>email: alexander\_merle@ph.tum.de

<sup>†</sup>email: werner\_rodejohann@ph.tum.de

# 1 Introduction

Neutrino physics aims to identify the form and origin of the neutrino mass matrix [1]. Towards this goal, literally dozens of new experiments are running, under construction or in development. For Majorana neutrinos, the neutrino mass matrix is given by

$$(m_\nu)_{\alpha\beta} = (U m_\nu^{\text{diag}} U^T)_{\alpha\beta} \quad \text{with } \alpha, \beta = e, \mu, \tau, \quad (1)$$

where  $m_\nu^{\text{diag}}$  is a diagonal matrix containing the three mass states  $m_{1,2,3}$ . In the basis in which the charged lepton mass matrix is real and diagonal,  $U$  is the leptonic mixing or PMNS matrix [2]. Being a symmetric matrix,  $m_\nu$  contains six independent and complex entries, corresponding to nine physical parameters. Several analyzes [3, 4, 5] have been performed in order to study the form of the neutrino mass matrix as allowed by current data. Reconstructing  $m_\nu$  is possible since for Majorana neutrinos – in contrast to the quark sector – the mass matrix is in general symmetric. In addition, the Majorana nature of neutrinos allows to probe an element of the mass matrix directly: namely, the second order weak interaction process  $(A, Z) \rightarrow (A, Z + 2) + 2e^-$ , denoted neutrino-less double beta decay ( $0\nu\beta\beta$ ), possesses a decay width proportional to the square of the so-called effective mass  $|m_{ee}| \equiv |\sum_i m_i U_{ei}^2|$ . In the charged lepton basis and if only the three light Majorana neutrinos as implied by the oscillation experiments are exchanged in  $0\nu\beta\beta$ , this coherent sum is nothing but the  $ee$  element of  $m_\nu$ . In order to experimentally reconstruct the mass matrix, the question arises if one can probe the other elements of  $m_\nu$  in the same sense as the  $ee$  element is probed by  $0\nu\beta\beta$ . In principle, the answer is “yes”: a mass matrix element  $m_{\alpha\beta}$  will govern  $\Delta L = 2$  lepton number violating processes with the charged leptons  $\alpha$  and  $\beta$  in the final state. For instance, the rare decay  $K^+ \rightarrow \pi^+ \mu^- \mu^-$  has a branching ratio proportional to  $|m_{\mu\mu}|^2$ , where  $m_{\mu\mu}$  is the  $\mu\mu$  entry of  $m_\nu$ . However, the possibility to probe the mass matrix by these decays is only academic, since neutrino oscillation data predicts branching ratios of such processes up to 20 orders of magnitude below current experimental limits [3, 6, 5].

Another, often studied aspect of mass matrices is the possibility of texture zeros, which can serve as a tool to explain certain properties of the observed mass and mixing schemes<sup>1</sup>. Models generating such texture zeros can be based on the Froggatt–Nielsen mechanism [10] or certain flavor symmetries [11]. Since texture zeros are very successful in the quark sector (see, e.g., [12] for a review), one expects such an approach to be useful for the lepton sector as well. It was found that in the charged lepton basis, and if neutrinos are Majorana particles, at most two zero entries in  $m_\nu$  are allowed [13, 14]<sup>2</sup>. Interesting and observable correlations between the neutrino mass and mixing parameters follow from the presence of two zeros. Regarding the possibility of just one zero entry in  $m_\nu$ , we are only aware of analyzes making simplifying assumptions such as a vanishing determinant [8] or the equality of two entries [16].

---

<sup>1</sup>The structure of  $m_\nu$  can also be constrained by assuming a vanishing determinant [7, 8] or a vanishing trace [9].

<sup>2</sup>For Dirac neutrinos there can be up to 5 zero entries [15].

In the present paper we wish to analyze the implications of vanishing mass matrix elements. Towards this goal, we study the individual mass matrix elements as functions of the smallest neutrino mass. Identifying the situations in which one of the entries can vanish, we obtain the phenomenological implications for the neutrino observables. This often concerns the  $ee$  element, i.e., the predictions for neutrino-less double beta decay are modified by the constraint of one of the  $m_{\alpha\beta}$  being zero. This modification concerns for instance the value of one of the Majorana phases, leading to little cancellation for the effective mass.

We parameterize the PMNS matrix as

$$U = \begin{pmatrix} c_{12}c_{13} & s_{12}c_{13} & s_{13}e^{-i\delta} \\ -s_{12}c_{23} - c_{12}s_{23}s_{13}e^{i\delta} & c_{12}c_{23} - s_{12}s_{23}s_{13}e^{i\delta} & s_{23}c_{13} \\ s_{12}s_{23} - c_{12}c_{23}s_{13}e^{i\delta} & -c_{12}s_{23} - s_{12}c_{23}s_{13}e^{i\delta} & c_{23}c_{13} \end{pmatrix} \text{diag}(1, e^{i\alpha}, e^{i(\beta+\delta)}), \quad (2)$$

where we have used the usual notations  $c_{ij} = \cos\theta_{ij}$ ,  $s_{ij} = \sin\theta_{ij}$  and  $\delta$  is the Dirac  $CP$ -violation phase, whereas  $\alpha$  and  $\beta$  are the two Majorana  $CP$ -violation phases [17]. In what regards the oscillation parameters, two independent mass squared differences,  $\Delta m_{\odot}^2 = m_2^2 - m_1^2$  and  $\Delta m_{\text{A}}^2 = |m_3^2 - m_1^2|$ , as well as three mixing angles are currently under examination. Their best-fit, 1 and  $3\sigma$  values are [18]

$$\begin{aligned} \Delta m_{\odot}^2 &= (7.9_{-0.3, 0.8}^{+0.3, 1.0}) \cdot 10^{-5} \text{ eV}^2, \\ \sin^2 \theta_{12} &= 0.31_{-0.03, 0.07}^{+0.02, 0.09}, \\ \Delta m_{\text{A}}^2 &= (2.2_{-0.27, 0.8}^{+0.37, 1.1}) \cdot 10^{-3} \text{ eV}^2, \\ \sin^2 \theta_{23} &= 0.50_{-0.05, 0.16}^{+0.06, 0.18}, \\ \sin^2 \theta_{13} &< 0.012 \text{ (0.046)}. \end{aligned} \quad (3)$$

The best-fit value for  $\sin^2 \theta_{13}$  is 0.

All six independent mass matrix elements depend crucially on the neutrino mass scheme, which is determined by the magnitude and the ordering (normal or inverted) of the individual neutrino masses:

$$\begin{aligned} \text{normal: } m_3 > m_2 > m_1 \quad &\text{with} \quad m_2 = \sqrt{m_1^2 + \Delta m_{\odot}^2}; \quad m_3 = \sqrt{m_1^2 + \Delta m_{\text{A}}^2}, \\ \text{inverted: } m_2 > m_1 > m_3 \quad &\text{with} \quad m_2 = \sqrt{m_3^2 + \Delta m_{\odot}^2 + \Delta m_{\text{A}}^2}; \quad m_1 = \sqrt{m_3^2 + \Delta m_{\text{A}}^2}. \end{aligned} \quad (4)$$

Of special interest are the following three extreme cases<sup>3</sup>:

$$\text{normal hierarchy (NH):} \quad |m_3| \simeq \sqrt{\Delta m_{\text{A}}^2} \gg |m_2| \simeq \sqrt{\Delta m_{\odot}^2} \gg |m_1|, \quad (5)$$

$$\text{inverted hierarchy (IH):} \quad |m_2| \simeq |m_1| \simeq \sqrt{\Delta m_{\text{A}}^2} \gg |m_3|, \quad (6)$$

$$\text{quasi-degeneracy (QD):} \quad m_0 \equiv |m_1| \simeq |m_2| \simeq |m_3| \gg \sqrt{\Delta m_{\text{A}}^2}. \quad (7)$$

---

<sup>3</sup>In the last case, QD, we denote with  $m_0$  the smallest neutrino mass, i.e., the definition written here applies for the normal ordering.

In the following Sections we will analyze the six independent mass matrix entries and study the implications of one of them being zero. It turns out that interesting implications from a texture zero in  $m_{ee}$  only occur for NH (see Section 2). If  $m_{e\mu}$  or  $m_{e\tau}$  should vanish, then this yields interesting correlations in case of IH and QD (see Section 3). The case of the  $\mu\mu$ ,  $\tau\tau$  and  $\mu\tau$  entries is studied in Section 4. Only for quasi-degenerate neutrino masses there are notable correlations, which interestingly affect the atmospheric neutrino mixing angle  $\theta_{23}$ . We conclude and summarize in Section 5.

## 2 The Mass Matrix Element $m_{ee}$

The  $ee$  entry of  $m_\nu$  has been the subject of intense investigation in the past [19] and we have nothing new to add here. For the sake of completeness, we nevertheless summarize the important features of  $m_{ee}$ . The current bound on  $|m_{ee}|$  is [20]

$$|m_{ee}| \leq 0.35 \zeta \text{ eV} , \quad (8)$$

where we have indicated with the factor  $\zeta = \mathcal{O}(1)$  the uncertainty due to the calculation of the nuclear matrix elements of  $0\nu\beta\beta$ . For an overview of the current status of  $0\nu\beta\beta$ , see [19, 21]. Given the fact that  $|m_{ee}|$  depends on 7 out of 9 parameters contained in the neutrino mass matrix (it neither depends on  $\delta$  nor on  $\theta_{23}$ ), it is obvious that a huge amount of information would be encoded in an observation of  $0\nu\beta\beta$ .

The effective mass  $|m_{ee}|$  reads in general and in the three extreme cases from Eqs. (5, 6, 7) as follows:

$$\begin{aligned} m_{ee} &= c_{13}^2 (m_1 c_{12}^2 + e^{2i\alpha} m_2 s_{12}^2) + e^{2i\beta} m_3 s_{13}^2 \\ \Rightarrow |m_{ee}| &\simeq \begin{cases} \left| e^{2i(\alpha-\beta)} \sqrt{\Delta m_\odot^2} c_{13}^2 s_{12}^2 + \sqrt{\Delta m_A^2} s_{13}^2 \right| & \text{NH,} \\ \sqrt{\Delta m_A^2} c_{13}^2 \sqrt{1 - \sin^2 2\theta_{12} \sin^2 \alpha} & \text{IH,} \\ m_0 |c_{12}^2 + e^{2i\alpha} s_{12}^2 + e^{2i\beta} s_{13}^2| & \text{QD.} \end{cases} \quad (9) \end{aligned}$$

A numerical evaluation of these expressions gives with best-fit,  $1\sigma$  and  $3\sigma$  values of the oscillation parameters for NH 2.8 (1.8–3.5, 0–6.2) meV, for IH 0.02–0.05 (0.01–0.05, 0.01–0.06) eV and for QD with  $m_0 = 0.5$  eV one gets 0.19–0.50 (0.16–0.51, 0.08–0.52) eV.

Interestingly, it will turn out that from all six independent entries in the mass matrix, the  $ee$  element as given in Eq. (9) looks most simple. Obviously, this has its reason in the simple form of the  $U_{ei}$  entries in the PMNS matrix, and is therefore a consequence of the chosen parametrization. For  $\theta_{13} = 0$  it is given by

$$(m_{ee})_{\theta_{13}=0} = m_1 c_{12}^2 + e^{2i\alpha} m_2 s_{12}^2 \Rightarrow |m_{ee}|_{\theta_{13}=0} \simeq \begin{cases} \sqrt{\Delta m_\odot^2} s_{12}^2 & \text{NH,} \\ \sqrt{\Delta m_A^2} \sqrt{1 - \sin^2 2\theta_{12} \sin^2 \alpha} & \text{IH,} \\ m_0 \sqrt{1 - \sin^2 2\theta_{12} \sin^2 \alpha} & \text{QD.} \end{cases} \quad (10)$$

The scale of  $m_{ee}$  for zero  $\theta_{13}$  and NH is roughly  $\sqrt{\Delta m_{\odot}^2} s_{12}^2 \simeq 0.003$  eV, for IH it is  $|m_{ee}| \simeq \sqrt{\Delta m_A^2} \simeq 0.04$  eV and for QD one has  $|m_{ee}| \simeq m_0$  (cancellations for IH and QD can be of order 50 %, though). Plugging in the best-fit values,  $1\sigma$  and  $3\sigma$  ranges,  $|m_{ee}|$  is given by 2.8 (2.4–3.0, 2.0–3.8) meV for NH, 17.8–46.9 (14.9–50.7, 7.5–57.4) meV for IH and, for QD with  $m_0 = 0.5$  eV, 0.19–0.50 (0.17–0.50, 0.10–0.50) eV. The Majorana phase  $\alpha$  is crucial for the magnitude of  $|m_{ee}|$  in case of IH and QD. When  $\sin \alpha = 0$ , then there is no cancellation, whereas for  $\sin \alpha = 1$  maximal cancellation occurs. Moreover,  $\sin \alpha = 0$  implies sizable instability with respect to radiative corrections. In Fig. 1 we show the  $ee$  element as a function of the smallest neutrino mass for four characteristic values of  $\theta_{13}$ . In this and some of the following plots we indicate a typical cosmological limit on the sum of neutrino masses  $\Sigma \equiv \sum m_i$  of 1.74 eV (thus  $m < 0.58$  eV for the lightest neutrino mass), obtained by an analysis of SDSS and WMAP data [22].

Turning to the possibility of texture zeros, it is well known that  $m_{ee} = 0$  is only possible for a limited parameter range in the normal mass ordering but for all values of  $\theta_{13}$  [23, 24]. As emphasized recently in [24], and reproduced here in Fig. 1, current data implies that not too large  $\theta_{13}$  values and  $m_1$  between  $10^{-3}$  and  $10^{-2}$  eV leads to vanishing  $|m_{ee}|$  (the “chimney”). For rather large  $\sin^2 2\theta_{13} \gtrsim 0.15$ , all values of  $m_1 \lesssim 0.01$  eV can lead to  $|m_{ee}| = 0$ . This implies values of the sum of neutrino masses smaller than current limits from cosmology, but merely one order of magnitude below. Next generation observations [25] will probe such values.

### 3 The Mass Matrix Elements $m_{e\mu}$ and $m_{e\tau}$

In general the  $e\mu$  element of  $m_\nu$  is given by

$$m_{e\mu} = c_{13} \left( (e^{2i\alpha} m_2 - m_1) s_{12} c_{12} c_{23} + e^{i\delta} (e^{2i\beta} m_3 - e^{2i\alpha} m_2 s_{12}^2 - m_1 c_{12}^2) s_{23} s_{13} \right). \quad (11)$$

Varying the three phases between  $-\pi$  and  $\pi$  and using the best-fit values and  $3\sigma$  ranges of the oscillation parameters as input we plot this element as a function of the smallest mass in Fig. 2.

It is always helpful to consider certain extreme cases. In this and the following Sections, we will analyze the cases  $\theta_{13} = 0$  and  $\theta_{23} = \pi/4$ .

- $\theta_{13} = 0$ :

$$(m_{e\mu})_{\theta_{13}=0} = (e^{2i\alpha} m_2 - m_1) s_{12} c_{12} c_{23} \quad (12)$$

This formula indicates that there is a lower limit on the  $e\mu$  element:

$$|m_{e\mu}|_{\theta_{13}=0} \gtrsim \begin{cases} s_{12} c_{12} c_{23} \sqrt{\Delta m_{\odot}^2} & \text{NH,} \\ s_{12} c_{12} c_{23} \frac{\Delta m_{\odot}^2}{2\sqrt{\Delta m_A^2}} & \text{IH,} \\ s_{12} c_{12} c_{23} \frac{\Delta m_{\odot}^2}{2m_0} & \text{QD.} \end{cases} \quad (13)$$

For the best-fit values this number is roughly 0.003 eV for NH, 0.0003 eV for IH, and for QD with  $m_0 = 0.5$  eV we have  $2.6 \cdot 10^{-5}$  eV. There is also an upper limit for IH and QD, reading  $2s_{12} c_{12} c_{23} \sqrt{\Delta m_A^2}$  and  $2s_{12} c_{12} c_{23} m_0$ , respectively. We conclude that for  $\theta_{13} = 0$  the  $e\mu$  entry can not vanish, but has a very low lower limit. Ignoring this small effect, we have

$$|m_{e\mu}|_{\theta_{13}=0} \simeq \begin{cases} \frac{1}{2} \sqrt{\Delta m_\odot^2} c_{23} \sin 2\theta_{12} & \text{NH,} \\ c_{23} \sin 2\theta_{12} \sqrt{\Delta m_A^2} \sin \alpha & \text{IH,} \\ m_0 c_{23} \sin 2\theta_{12} \sin \alpha & \text{QD.} \end{cases} \quad (14)$$

The scale of  $m_{e\mu}$  for zero  $\theta_{13}$  and NH is roughly  $\sqrt{\Delta m_\odot^2}/\sqrt{8} \simeq 0.002$  eV, for IH and QD there can be almost total cancellation. Numerically, we have for the best-fit values and the 1 and  $3\sigma$  ranges 2.9 (2.6–3.2, 2.0–3.8) meV for NH, 0–30.7 (0–35.4, 0–45.7) meV for IH and for QD with  $m_0 = 0.5$  eV one gets 0–0.33 (0–0.35, 0–0.40) eV. The range for  $m_{e\mu}$  in case of IH and QD is much larger than for NH, because – in addition to the oscillation parameters – the mass matrix element is proportional to  $\sin \alpha$ .

- $\theta_{23} = \pi/4$ :

$$(m_{e\mu})_{\theta_{23}=\pi/4} = \frac{c_{13}}{\sqrt{2}} \left( (e^{2i\alpha} m_2 - m_1) s_{12} c_{12} + e^{i\delta} (e^{2i\beta} m_3 - e^{2i\alpha} m_2 s_{12}^2 - m_1 c_{12}^2) s_{13} \right)$$

$$\Rightarrow |m_{e\mu}|_{\theta_{23}=\pi/4} \simeq \begin{cases} \frac{c_{13}}{\sqrt{2}} \left| e^{2i\alpha} \sqrt{\Delta m_\odot^2} s_{12} c_{12} + e^{i\delta} \left( e^{2i\beta} \sqrt{\Delta m_A^2} - e^{2i\alpha} \sqrt{\Delta m_\odot^2} s_{12}^2 \right) s_{13} \right| & \text{NH,} \\ \sqrt{\Delta m_A^2} \frac{c_{13}}{\sqrt{2}} \left| (e^{2i\alpha} - 1) c_{12} s_{12} - e^{i\delta} (c_{12}^2 + e^{2i\alpha} s_{12}^2) s_{13} \right| & \text{IH,} \\ m_0 \frac{c_{13}}{\sqrt{2}} \left| (e^{2i\alpha} - 1) c_{12} s_{12} + e^{i\delta} (e^{2i\beta} - c_{12}^2 - e^{2i\alpha} s_{12}^2) s_{13} \right| & \text{QD.} \end{cases} \quad (15)$$

Numerically, we have for the best-fit values and the 1 and  $3\sigma$  ranges 2.9 (0–7.1, 0–12.3) meV for NH, 0–30.7 (0–34.8, 0–40.6) meV for IH and for QD with  $m_0 = 0.5$  eV one gets 0–0.33 (0–0.38, 0–0.43) eV. In Fig. 2 one can see that for NH and the best-fit oscillation parameters the value  $\sin^2 2\theta_{13} = 0.03$  allows for complete cancellation for all allowed values of  $m_1$ . When  $m_1$  is negligible, this can be understood by noting that when  $\sin^2 2\theta_{13} = 0.03$ , the two leading terms in the formula Eq. (15), namely  $\sqrt{\Delta m_\odot^2} s_{12} c_{12}$  and  $\sqrt{\Delta m_A^2} s_{13}$ , happen to be almost identical. For smaller (larger)  $\theta_{13}$  the first (second) term dominates and no cancellation for hierarchical neutrinos is possible. In case of IH and QD the  $e\mu$  element can always vanish. This requires the first term in Eq. (15) to be small, thereby implying  $\sin \alpha \simeq 0$ , which leads to little cancellation in  $0\nu\beta\beta$  (see Eq. (9)):

$$|m_{ee}|_{\theta_{13} \neq 0}^{m_{e\mu}=0} \simeq \begin{cases} \sqrt{\Delta m_A^2} c_{13}^2 & \text{IH,} \\ m_0 c_{13}^2 & \text{QD.} \end{cases} \quad (16)$$

We plot in Fig. 3 the correlation between some of the observables which result if  $m_{e\mu} = 0$ . All oscillation parameters are varied in their  $3\sigma$  ranges. The upper plot is a scatter plot

of the smallest mass against the Majorana phase  $\alpha$  for both mass orderings. As expected from the above considerations, for an inverted ordering and for quasi-degenerate masses  $\sin \alpha$  is very small. Consequently, the effective mass is basically given by  $\sqrt{\Delta m_A^2}$  or  $m_0$  and the gap between the maximal effective mass for NH and the minimal effective mass for IH is sizably larger than without the restriction  $m_{e\mu} = 0$  (cf. the lower plot of Fig. 3 with Fig. 1). The small band of values of  $|m_{ee}|$  for large masses is a consequence of  $\sin \alpha \simeq 0$ . Note that  $m_{ee}$  and  $m_{e\mu}$  can vanish simultaneously [13, 14]. The resulting correlation of parameters in this case and in all other allowed two zero cases is for the sake of completeness reproduced in Table 1.

The results for the  $e\tau$  element of  $m_\nu$  are very similar to the ones for  $m_{e\mu}$ : the explicit form of  $m_{e\tau}$  is

$$m_{e\tau} = c_{13} \left( (m_1 - e^{2i\alpha} m_2) s_{12} c_{12} s_{23} + e^{i\delta} (e^{2i\beta} m_3 - e^{2i\alpha} m_2 s_{12}^2 - m_1 c_{12}^2) c_{23} s_{13} \right), \quad (17)$$

i.e., it is obtained from  $m_{e\mu}$  by exchanging  $s_{23}$  with  $c_{23}$  and  $c_{23}$  with  $-s_{23}$ . A plot of  $m_{e\tau}$  against the smallest neutrino mass is basically indistinguishable from the plot of  $m_{e\mu}$  against the smallest mass. This is the obvious consequence of the (approximate)  $\mu$ - $\tau$  exchange symmetry [26] of the neutrino mass matrix in the charged lepton basis.

## 4 The Mass Matrix Elements $m_{\mu\mu}$ , $m_{\tau\tau}$ and $m_{\mu\tau}$

The  $\mu\mu$  entry of the mass matrix reads

$$m_{\mu\mu} = m_1 (c_{23} s_{12} + e^{i\delta} c_{12} s_{13} s_{23})^2 + e^{2i\alpha} m_2 (c_{12} c_{23} - e^{i\delta} s_{12} s_{13} s_{23})^2 + e^{2i(\beta+\delta)} m_3 c_{13}^2 s_{23}^2. \quad (18)$$

In Fig. 4 we plot this element as a function of the smallest neutrino mass for both mass orderings and for the best-fit values and  $3\sigma$  ranges of the oscillation parameters.

Let us again analyze the form of  $m_{\mu\mu}$  in our two special cases:

- $\theta_{13} = 0$ :

$$(m_{\mu\mu})_{\theta_{13}=0} = c_{23}^2 (e^{2i\alpha} m_2 c_{12}^2 + m_1 s_{12}^2) + e^{2i(\beta+\delta)} m_3 s_{23}^2$$

$$\Rightarrow |m_{\mu\mu}|_{\theta_{13}=0} \simeq \begin{cases} s_{23} \sqrt{\Delta m_A^2 s_{23}^2 + 2\sqrt{\Delta m_\odot^2 \Delta m_A^2} c_{12}^2 c_{23}^2 c_{2(\alpha-\beta-\delta)}} & \text{NH,} \\ \sqrt{\Delta m_A^2} c_{23}^2 \sqrt{1 - \sin^2 2\theta_{12} \sin^2 \alpha} & \text{IH,} \\ m_0 |c_{23}^2 (e^{2i\alpha} c_{12}^2 + s_{12}^2) + e^{2i(\beta+\delta)} s_{23}^2| & \text{QD.} \end{cases} \quad (19)$$

The scale of  $m_{\mu\mu}$  for zero  $\theta_{13}$  and NH is roughly  $\sqrt{\Delta m_A^2}/2 \simeq 0.02$  eV. For IH it is approximately the same value, but cancellations up to 50 % are possible. For QD there can be complete cancellation, which we will discuss below. Numerically, for the



best-fit values and the 1 and  $3\sigma$  ranges, we have 20.2–26.3 (15.8–31.1, 6.4–41.3) meV for NH, 8.9–23.5 (6.6–27.9, 2.4–37.9) meV for IH. For QD with  $m_0 = 0.5$  eV it holds 0.0–0.5 (0–0.5, 0–0.5) eV. inverted ordering. Actually, there is a slight difference between normal and inverted ordering if neutrinos are quasi-degenerate in mass, see below.

For zero  $\theta_{13}$  the element  $m_{\mu\mu}$  cannot vanish for NH and IH. For NH and the best-fit values, the  $\mu\mu$  entry has only a rather small range, centered around  $\sqrt{\Delta m_A^2}/2$ . The value of  $m_{\mu\mu}$  is in case of IH nothing but the effective mass  $|m_{ee}|$  multiplied with  $c_{23}^2$ . If  $\alpha = 0$  then  $m_{\mu\mu}$  takes its maximal value  $\sqrt{\Delta m_A^2} c_{23}^2 = c_{23}^2 |m_{ee}|$ . Moreover, as shown in Section 3, the  $e\mu$  and  $e\tau$  elements are very small in this case. If neutrinos are quasi-degenerate, Eq. (19) indicates that  $m_{\mu\mu}$  vanishes if  $c_{23}^2 (e^{2i\alpha} c_{12}^2 + s_{12}^2) + e^{2i(\beta+\delta)} s_{23}^2$  vanishes. In case of  $\theta_{23} = \pi/4$  this expression is zero for  $\sin \alpha = 0$  and  $\sin(\beta + \delta) = 1$ . Looking at Fig. 4, however, one sees that for vanishing  $\theta_{13}$  the curve for minimal  $|m_{\mu\mu}|$  and normal ordering does not coincide with the one for inverted ordering, and in addition is non-zero. To understand this, let us define  $2r_\odot \equiv \Delta m_\odot^2/m_0^2$  and  $2r_A \equiv \Delta m_A^2/m_0^2$ , which allows from Eq. (4) to write  $m_1 = m_0$ ,  $m_3 \simeq m_0(1 + r_A)$  and  $m_2 \simeq m_0(1 + r_\odot)$  for the normal ordering and  $m_3 = m_0$ ,  $m_1 \simeq m_0(1 + r_A)$  and  $m_2 \simeq m_0(1 + r_A + r_\odot)$  for the inverted ordering. Within this approximation, the formulae for  $m_{\mu\mu}$  in case of normal and inverted ordering read:

$$(m_{\mu\mu})_{\theta_{23}=\pi/4, \theta_{13}=0}^{\text{QD}} \simeq \begin{cases} \frac{1}{2}m_0 (s_{12}^2 + c_{12}^2 e^{2i\alpha} (1 + r_\odot) + e^{2i(\beta+\delta)} (1 + r_A)) & \text{normal,} \\ \frac{1}{2}m_0 (s_{12}^2 (1 + r_A) + c_{12}^2 e^{2i\alpha} (1 + r_A + r_\odot) + e^{2i(\beta+\delta)}) & \text{inverted.} \end{cases} \quad (20)$$

For both possibilities, the term proportional to  $e^{2i(\beta+\delta)}$  dominates the other two. However, for the inverted ordering the sum of the two remaining terms can exceed the contribution from the third, leading term. Hence, the  $\mu\mu$  entry can vanish for the inverted ordering. In case of normal ordering, however, the sum of the two sub-leading terms is always smaller than the third, leading term and therefore the minimal value of the  $\mu\mu$  element is non-zero. For  $m_0 = 0.3$  eV it is given by  $\frac{1}{2}m_0 ((1 + r_A) - c_{12}^2 (1 + r_A + r_\odot) - s_{12}^2) = \frac{1}{2}m_0 (r_A - c_{12}^2 r_\odot) \simeq 0.0018$  eV. This agrees well with the value in Fig. 4. Note also that from Eq. (20) one finds that the minimal values of  $m_{\mu\mu}$  are different for normal and inverted ordering, with this difference given also by  $\frac{1}{2}m_0 (r_A - c_{12}^2 r_\odot)$ . This is in contrast to  $m_{ee}$ ,  $m_{e\mu}$  and  $m_{e\tau}$ , which show no such difference for neutrino masses larger than 0.1 eV. It is easy to show that, for  $\theta_{13} = 0$ , the difference between the minimal value of  $m_{ee}$  for normal and inverted ordering is of order  $m_0 r_A$ . However, since the minimal value of  $|m_{ee}|$  is much larger than this difference (namely of the order  $m_0 \cos 2\theta_{12}$ ), the difference cannot be seen in Fig. 1. For  $m_{e\mu}$  and  $m_{e\tau}$  it turns out that the difference between the minimal values for normal and inverted ordering vanishes.

Nevertheless, the approximate expression for QD in Eq. (19) indicates the presence of an interesting correlation between  $\alpha$  and  $\theta_{23}$ , obtained when one requires the  $\mu\mu$  entry to vanish. At the end of this Section we will study this in detail.



- $\theta_{23} = \pi/4$ :

$$(m_{\mu\mu})_{\theta_{23}=\pi/4} = \frac{1}{2}m_1 (s_{12} + e^{i\delta} c_{12} s_{13})^2 + e^{2i\alpha} m_2 (c_{12} - e^{i\delta} s_{12} s_{13})^2 + e^{2i(\beta+\delta)} m_3 c_{13}^2$$

$$\Rightarrow |m_{\mu\mu}|_{\theta_{23}=\pi/4} \simeq \begin{cases} \frac{1}{2} c_{13}^2 \sqrt{\Delta m_A^2} \sqrt{\Delta m_A^2 c_{13}^2 + 2\sqrt{\Delta m_\odot^2 \Delta m_A^2} c_{12}^2 c_{2(\alpha-\beta-\delta)}} & \text{NH,} \\ \frac{1}{2} \sqrt{\Delta m_A^2} |e^{2i\alpha} c_{12}^2 + s_{12}^2 + 2e^{i\delta} (1 - e^{2i\alpha}) c_{12} s_{12} s_{13}| & \text{IH,} \\ \frac{1}{2} m_0 |e^{2i\alpha} c_{12}^2 + s_{12}^2 + e^{2i(\beta+\delta)} c_{13}^2 + 2e^{i\delta} (1 - e^{2i\alpha}) c_{12} s_{12} s_{13}| & \text{QD.} \end{cases} \quad (21)$$

Numerically, one gets 0.9–1.2 (0.8–1.4, 0.1–1.8) meV for NH, 8.9–23.5 (2.9–25.9, 0–31.3) meV for IH and for QD with  $m_0 = 0.5$  eV we have 0–0.50 eV (0–0.50 eV, 0–0.51 eV). Comparing the expressions with the case of vanishing  $\theta_{13}$  in Eq. (19) we see that the corrections are rather small. One notable difference is that  $m_{\mu\mu}$  can vanish now for IH.

Again, the (approximate)  $\mu$ - $\tau$  symmetry implies that  $m_{\mu\mu} \simeq m_{\tau\tau}$ . The explicit form of  $m_{\tau\tau}$  is

$$m_{\tau\tau} = m_1 (e^{i\delta} c_{12} s_{13} c_{23} - s_{23} s_{12})^2 + e^{2i\alpha} m_2 (c_{12} s_{23} + e^{i\delta} s_{12} s_{13} c_{23})^2 + e^{2i(\beta+\delta)} m_3 c_{13}^2 c_{23}^2. \quad (22)$$

It is obtained from  $m_{\mu\mu}$  by exchanging  $s_{23}$  with  $c_{23}$  and  $c_{23}$  with  $-s_{23}$ . The mass matrix element  $m_{\mu\tau}$  reads:

$$|m_{\mu\tau}| = \frac{1}{2} \cos 2\theta_{23} e^{i\delta} (m_1 - e^{2i\alpha} m_2) \sin 2\theta_{12} s_{13} - \frac{1}{2} \sin 2\theta_{23} (e^{2i\alpha} m_2 c_{12}^2 + m_1 s_{12}^2 - e^{2i\delta} (e^{2i\beta} m_3 c_{13}^2 + (m_1 c_{12}^2 + e^{2i\alpha} m_2 s_{12}^2) s_{13}^2)) \quad (23)$$

The first term is suppressed by the close-to-maximal  $\theta_{23}$  and the smallness of  $\theta_{13}$ . One can show that  $m_{\mu\tau}$  is obtained from  $m_{\mu\mu}$  by exchanging  $c_{23}^2$  with  $-c_{23} s_{23}$ ,  $s_{23}^2$  with  $c_{23} s_{23}$  and  $c_{23} s_{23}$  with  $1/2 (c_{23}^2 - s_{23}^2)$ . A plot of  $|m_{\mu\tau}|$  as a function of the smallest mass is given in Fig. 5 and looks rather similar to the cases of  $|m_{\mu\mu}|$  and  $|m_{\tau\tau}|$ . Note that for  $\theta_{13} = 0$  the minimal values for the normal and inverted ordering show differences. Moreover, for the normal mass ordering and quasi-degenerate masses  $m_{\mu\tau}$  cannot vanish when  $\theta_{13} = 0$ . This can be explained in analogy to the issues discussed above for  $m_{\mu\mu}$ . Non-zero  $\theta_{13}$  and normal ordering allow for zero  $m_{\mu\tau}$  only in the QD regime. In case of IH, the  $\mu\tau$  entry can not vanish.

It is clear from the above discussion that an interesting correlation in case of a vanishing  $\mu\mu$ ,  $\mu\tau$  or  $\tau\tau$  element can occur only if neutrinos are quasi-degenerate. Let us summarize the form of the three relevant mass matrix elements for QD:

$$\begin{aligned} |m_{\mu\mu}|^{\text{QD}} &\simeq m_0 |c_{23}^2 (e^{2i\alpha} c_{12}^2 + s_{12}^2) + e^{2i(\beta+\delta)} s_{23}^2|, \\ |m_{\tau\tau}|^{\text{QD}} &\simeq m_0 |s_{23}^2 (e^{2i\alpha} c_{12}^2 + s_{12}^2) + e^{2i(\beta+\delta)} c_{23}^2|, \\ |m_{\mu\tau}|^{\text{QD}} &\simeq m_0 c_{23} s_{23} |(e^{2i\alpha} c_{12}^2 + s_{12}^2) - e^{2i(\beta+\delta)}|. \end{aligned} \quad (24)$$

Recall that for  $\theta_{13} = 0$  the  $\mu\tau$  element cannot vanish if neutrinos are normally ordered. Including finite values of  $\theta_{13}$  will lead to modifications of the order  $\sin\theta_{13}$  in the above formulae. It is apparent that correlations between the phases and  $\theta_{23}$  are implied. For the  $\mu\mu$  entry we can immediately see from Eq. (24) that for  $\theta_{23} > \pi/4$  the mass matrix element cannot vanish. Consequently, a vanishing  $\tau\tau$  element is not possible for  $\theta_{23} < \pi/4$ . However, finite values of  $\theta_{13}$  will allow for values of  $\theta_{23}$  slightly below (above)  $\pi/4$ . Exactly maximal  $\theta_{23} = \pi/4$  will lead to vanishing  $\mu\mu$  or  $\tau\tau$  entries if  $\sin\alpha = 0$  and  $\sin(\beta + \delta) = 1$ . For the  $\mu\tau$  entry there is no dependence on  $\theta_{23}$ , and  $m_{\mu\tau} = 0$  is only possible for values of the phases corresponding to  $\sin\alpha = \sin(\beta + \delta) = 0$ . In Fig. 6 we show for two values of  $\theta_{13}$  scatter plots of  $\alpha$  against  $\sin^2\theta_{23}$  and of  $\beta + \delta$  against  $\sin^2\theta_{23}$ , confirming these considerations.

We see in particular that close-to-maximal atmospheric mixing implies small  $\sin\alpha$ , which indicates very little cancellation in the effective mass. In Fig. 7 we give scatter plots of the smallest mass against  $|m_{ee}|$ , obtained by demanding  $m_{\mu\mu}$  and  $m_{\mu\tau}$  to vanish and by varying the oscillation parameters within their  $3\sigma$  ranges. In case of an inverted ordering,  $m_{\mu\mu} = 0$  is possible for all masses, whereas  $m_{\mu\tau} = 0$  works only for  $m_3 \gtrsim 0.01$  eV. Note that  $m_{ee} = 0$  will not be possible if  $m_{\mu\mu}$ ,  $m_{\mu\tau}$  or  $m_{\tau\tau}$  also vanish [13, 14]. For normal ordering,  $m_{\mu\mu} = 0$  is possible when  $m_1 \gtrsim 0.02$  eV, whereas  $m_{\mu\tau} = 0$  works only for  $m_1 \gtrsim 0.1$  eV. The small band of values of  $|m_{ee}|$  for large masses is a consequence of  $\sin\alpha \simeq 0$ .

As summarized in Table 1,  $m_{\mu\mu}$  and  $m_{\mu\tau}$  can vanish simultaneously. Also  $m_{\mu\mu}$  and  $m_{e\mu}$  (or  $m_{e\tau}$ ) and  $m_{\tau\tau}$  and  $m_{e\mu}$  (or  $m_{e\tau}$ ) can vanish at the same time. Vanishing of  $m_{\mu\tau}$  will only be possible if no other entry of  $m_\nu$  is zero.

## 5 Conclusions and Summary

We have studied the allowed ranges of the individual mass matrix elements in the charged lepton basis. Areas of parameter space in which they can vanish have been analyzed, their phenomenological consequences have been studied and a limited number of correlations has been found. Let us summarize the main features:

- the  $ee$  element, or the effective mass, can vanish for all values of  $\theta_{13}$ , but only for small values of  $m_1$  in the normal mass ordering. As a function of the smallest neutrino mass, it has from all six independent elements the most interesting structure;
- the  $e\mu$  and  $e\tau$  entries are very much alike. If  $\theta_{13} = 0$ , they can not vanish. For non-zero  $\theta_{13}$  there can be a texture zero for all mass values. However, the inverted hierarchy and the quasi-degenerate spectrum require that  $\sin\alpha \simeq 0$ , which implies little cancellation in the effective mass;
- the  $\mu\mu$  and  $\tau\tau$  entries are also very much alike. In case of  $\theta_{13} = 0$ , vanishing is only possible for a smallest mass larger than  $\simeq 0.01$  eV. For non-zero  $\theta_{13}$  and normal ordering, zero entries also require that  $m_1 \gtrsim 0.01$  eV, whereas for an inverted ordering all mass values allow for complete cancellation. For quasi-degenerate masses,  $\theta_{23}$  lies

below  $\pi/4$  if  $m_{\mu\mu} = 0$  and above  $\pi/4$  if  $m_{\tau\tau} = 0$ . Again,  $\sin \alpha \simeq 0$  is required, which translates into little cancellation for  $|m_{ee}|$ ;

- the  $\mu\tau$  entry cannot vanish if  $\theta_{13} = 0$  and the masses are normally ordered. Non-zero  $\theta_{13}$  and normal ordering allows for zero  $m_{\mu\tau}$  if  $m_1 \gtrsim 0.1$  eV, but  $m_3$  can be larger than a few times 0.001 eV for an inverted ordering. Vanishing in case of NH or IH is not possible. Again, for quasi-degenerate neutrinos  $\sin \alpha \simeq 0$  is required, which translates into little cancellation for  $|m_{ee}|$ .

We finish by stressing once more that typically the requirement of a vanishing element (except for  $m_{ee}$ , of course) leads to little cancellation for the effective mass.

### Acknowledgments:

This work has been supported by the “Deutsche Forschungsgemeinschaft” in the “Sonderforschungsbereich 375 für Astroteilchenphysik” (A.M. and W.R.) and under project number RO-2516/3-1 (W.R.).

## References

- [1] R. N. Mohapatra *et al.*, hep-ph/0412099; hep-ph/0510213.
- [2] B. Pontecorvo, Zh. Eksp. Teor. Fiz. **33**, 549 (1957) and **34**, 247 (1957); Z. Maki, M. Nakagawa and S. Sakata, Prog. Theor. Phys. **28**, 870 (1962).
- [3] W. Rodejohann, Phys. Rev. D **62**, 013011 (2000); J. Phys. G **28**, 1477 (2002).
- [4] M. Frigerio and A. Y. Smirnov, Nucl. Phys. B **640**, 233 (2002); Phys. Rev. D **67**, 013007 (2003).
- [5] A. Atre, V. Barger and T. Han, Phys. Rev. D **71**, 113014 (2005).
- [6] K. Zuber, hep-ph/0008080; C. S. Lim, E. Takasugi and M. Yoshimura, Prog. Theor. Phys. **113**, 1367 (2005); A. Ali, A. V. Borisov and N. B. Zamorin, Eur. Phys. J. C **21**, 123 (2001).
- [7] G. C. Branco *et al.*, Phys. Lett. B **562**, 265 (2003).
- [8] Z. Z. Xing, Phys. Rev. D **69**, 013006 (2004); B. C. Chauhan, J. Pulido and M. Picariello, Phys. Rev. D **73**, 053003 (2006).
- [9] D. Black, A. H. Fariborz, S. Nasri and J. Schechter, Phys. Rev. D **62**, 073015 (2000); X. G. He and A. Zee, Phys. Lett. B **560**, 87 (2003); Phys. Rev. D **68**, 037302 (2003); W. Rodejohann, Phys. Lett. B **579**, 127 (2004); S. Nasri, J. Schechter and S. Moussa, Phys. Rev. D **70**, 053005 (2004); Phys. Rev. D **71**, 093005 (2005).

- [10] C. D. Froggatt and H. B. Nielsen, Nucl. Phys. B **147**, 277 (1979).
- [11] See for instance W. Grimus *et al.*, Eur. Phys. J. C **36**, 227 (2004).
- [12] H. Fritzsch and Z. Z. Xing, Prog. Part. Nucl. Phys. **45**, 1 (2000).
- [13] P. H. Frampton, S. L. Glashow and D. Marfatia, Phys. Lett. B **536**, 79 (2002).
- [14] Z. Z. Xing, Phys. Lett. B **530**, 159 (2002); B. R. Desai, D. P. Roy and A. R. Vaucher, Mod. Phys. Lett. A **18**, 1355 (2003); W. L. Guo and Z. Z. Xing, Phys. Rev. D **67**, 053002 (2003); see also S. K. Kang and C. S. Kim, Phys. Rev. D **63**, 113010 (2001).
- [15] C. Hagedorn and W. Rodejohann, JHEP **0507**, 034 (2005).
- [16] S. Kaneko, H. Sawanaka and M. Tanimoto, JHEP **0508**, 073 (2005).
- [17] S. M. Bilenky, J. Hosek and S. T. Petcov, Phys. Lett. B **94**, 495 (1980); M. Doi *et al.*, Phys. Lett. B **102**, 323 (1981); J. Schechter and J. W. F. Valle, Phys. Rev. D **23**, 1666 (1981).
- [18] M. Maltoni, T. Schwetz, M. A. Tortola and J. W. F. Valle, New J. Phys. **6**, 122 (2004).
- [19] S. T. Petcov, New J. Phys. **6**, 109 (2004) and references therein.
- [20] H. V. Klapdor-Kleingrothaus *et al.*, Eur. Phys. J. A **12**, 147 (2001); C. E. Aalseth *et al.* [IGEX Collaboration], Phys. Rev. D **65**, 092007 (2002).
- [21] C. Aalseth *et al.*, hep-ph/0412300 and references therein.
- [22] M. Tegmark *et al.*, Phys. Rev. D **69**, 103501 (2004).
- [23] S. Pascoli, S. T. Petcov and L. Wolfenstein, Phys. Lett. B **524**, 319 (2002); Z. Z. Xing, Phys. Rev. D **68**, 053002 (2003); S. Choubey and W. Rodejohann, Phys. Rev. D **72**, 033016 (2005).
- [24] M. Lindner, A. Merle and W. Rodejohann, Phys. Rev. D **73**, 053005 (2006).
- [25] For an overview see S. Hannestad, Nucl. Phys. Proc. Suppl. **145**, 313 (2005), hep-ph/0412181.
- [26] C. S. Lam, Phys. Lett. B **507**, 214 (2001); W. Grimus and L. Lavoura, JHEP **0107**, 045 (2001); E. Ma, Phys. Rev. D **66**, 117301 (2002); P. F. Harrison and W. G. Scott, Phys. Lett. B **547**, 219 (2002); an incomplete list of more recent studies is: Y. Koide, Phys. Rev. D **69**, 093001 (2004); W. Grimus *et al.*, Nucl. Phys. B **713**, 151 (2005); R. N. Mohapatra, JHEP **0410**, 027 (2004); I. Aizawa, T. Kitabayashi and M. Yasue, Phys. Rev. D **72**, 055014 (2005); C. S. Lam, Phys. Rev. D **71**, 093001 (2005); R. N. Mohapatra and W. Rodejohann, Phys. Rev. D **72**, 053001 (2005); A. S. Joshipura, hep-ph/0512252; Y. H. Ahn *et al.*, hep-ph/0602160.

Matrix	Correlation
$\begin{pmatrix} 0 & 0 & a \\ 0 & b & d \\ a & d & e \end{pmatrix}$	only NH $ U_{e3}  \simeq \frac{\sqrt{R}}{2} \cot \theta_{23} \frac{\sin 2\theta_{12}}{\sqrt{\cos 2\theta_{12}}}$
$\begin{pmatrix} 0 & a & 0 \\ a & b & d \\ 0 & d & e \end{pmatrix}$	only NH $ U_{e3}  \simeq \frac{\sqrt{R}}{2} \tan \theta_{23} \frac{\sin 2\theta_{12}}{\sqrt{\cos 2\theta_{12}}}$
$\begin{pmatrix} a & 0 & b \\ 0 & 0 & d \\ b & d & e \end{pmatrix}$	QD; both orderings $ U_{e3}  \simeq \frac{R}{2} \left  \frac{\cot 2\theta_{23}}{\cos \delta} \right  \sin 2\theta_{12}$
$\begin{pmatrix} a & b & 0 \\ b & 0 & d \\ 0 & d & e \end{pmatrix}$	same as above
$\begin{pmatrix} a & b & 0 \\ b & d & e \\ 0 & e & 0 \end{pmatrix}$	QD; both orderings $ U_{e3}  \simeq \frac{R}{2} \left  \frac{\tan 2\theta_{23}}{\cos \delta} \right  \sin 2\theta_{12}$
$\begin{pmatrix} a & 0 & b \\ 0 & d & e \\ b & e & 0 \end{pmatrix}$	same as above
$\begin{pmatrix} a & b & d \\ b & 0 & e \\ d & e & 0 \end{pmatrix}$	QD; both orderings $ U_{e3}  \simeq \frac{\cot 2\theta_{12} \cot 2\theta_{23}}{\cos \delta}$

Table 1: Mass matrices with two zeros and the resulting correlations [13, 14].

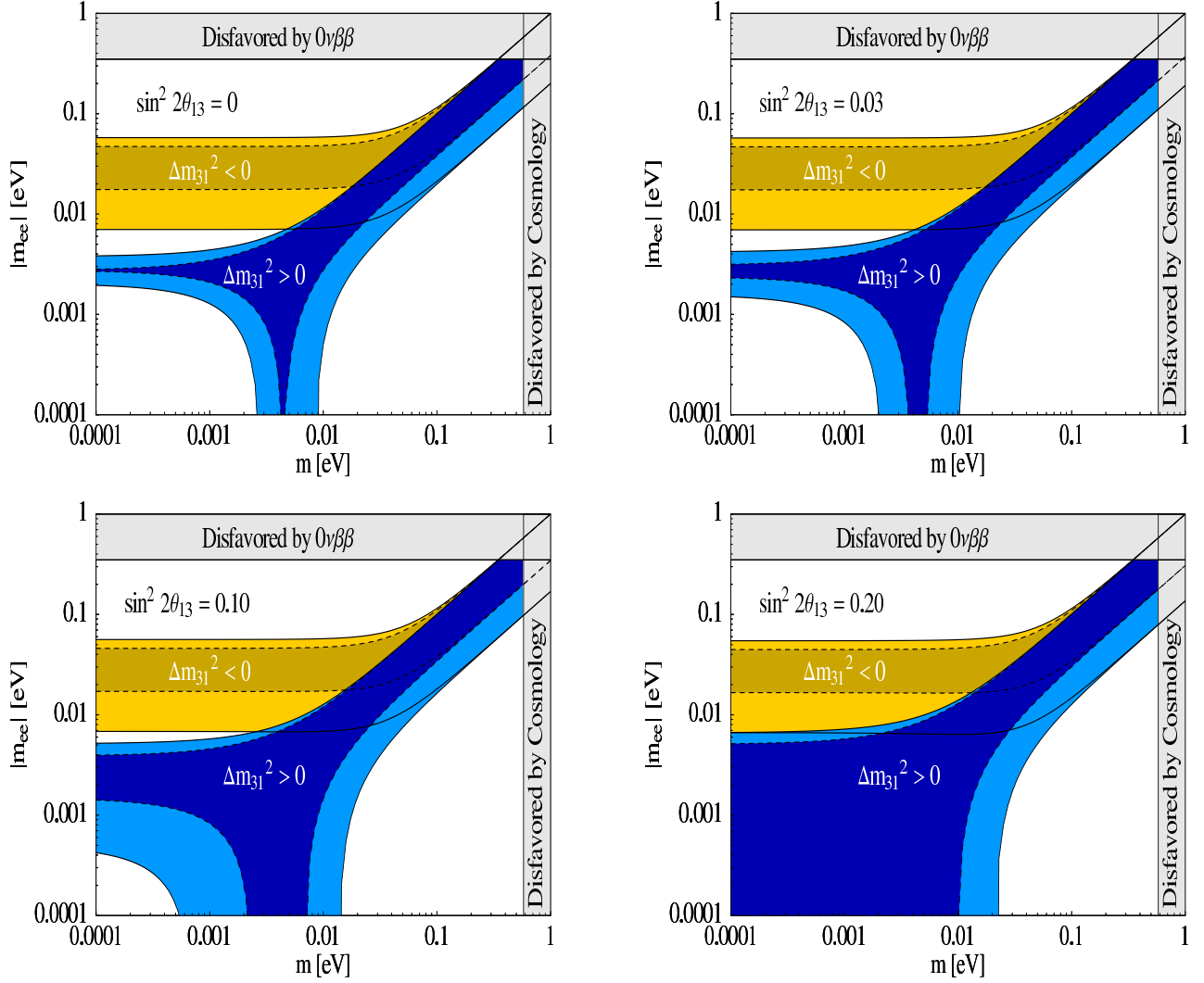


Figure 1: The absolute value of the mass matrix element  $m_{ee}$  against the smallest neutrino mass for the normal and inverted mass ordering for four representative values of  $\theta_{13}$ . The best-fit and  $3\sigma$  ranges of the oscillation parameters are used.

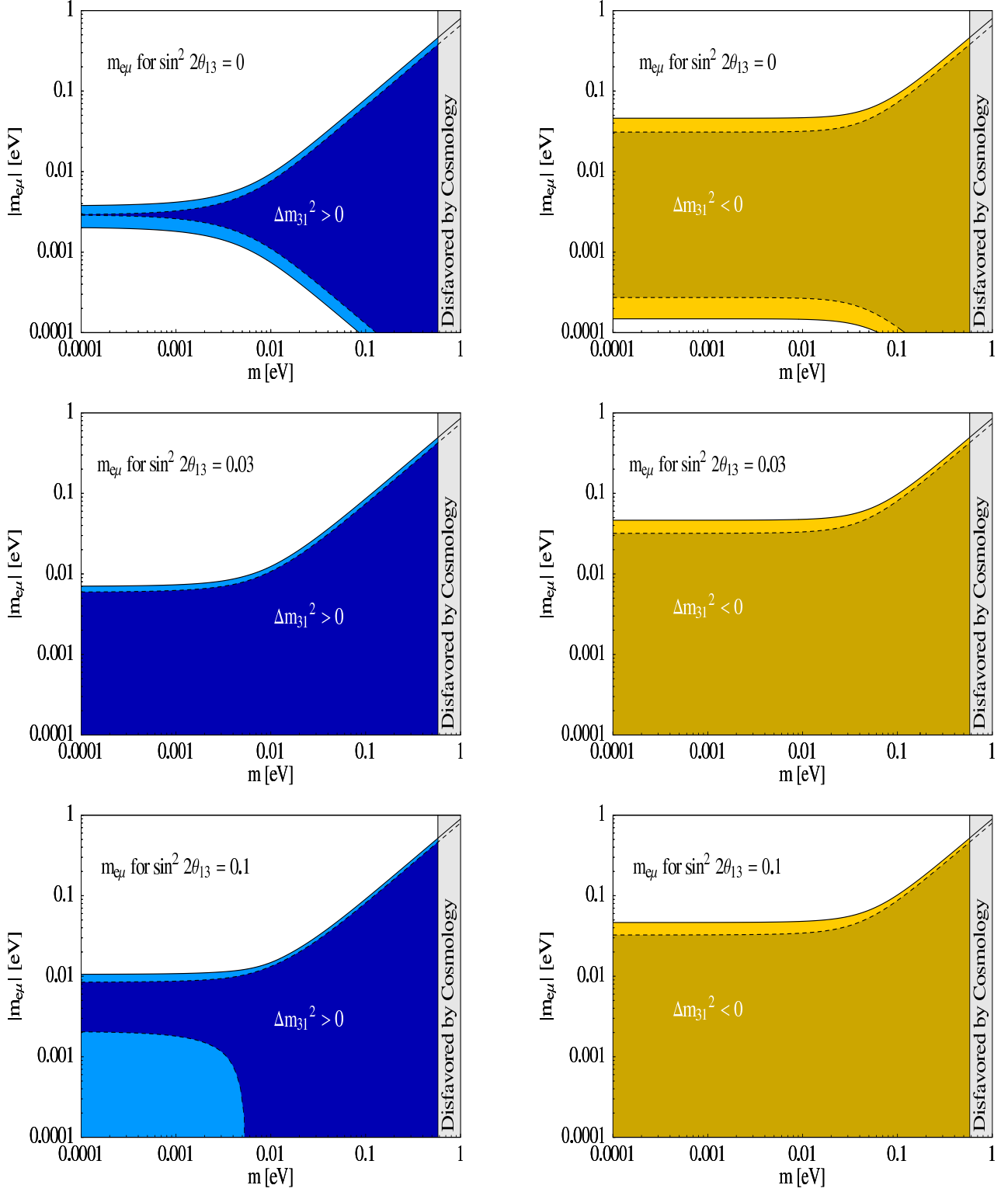


Figure 2: The absolute value of the mass matrix element  $m_{e\mu}$  against the smallest neutrino mass for the normal and inverted mass ordering for three representative values of  $\theta_{13}$ . The normal (inverted) mass ordering is given on the left (right) side. The corresponding plot for  $m_{e\tau}$  looks basically identical.



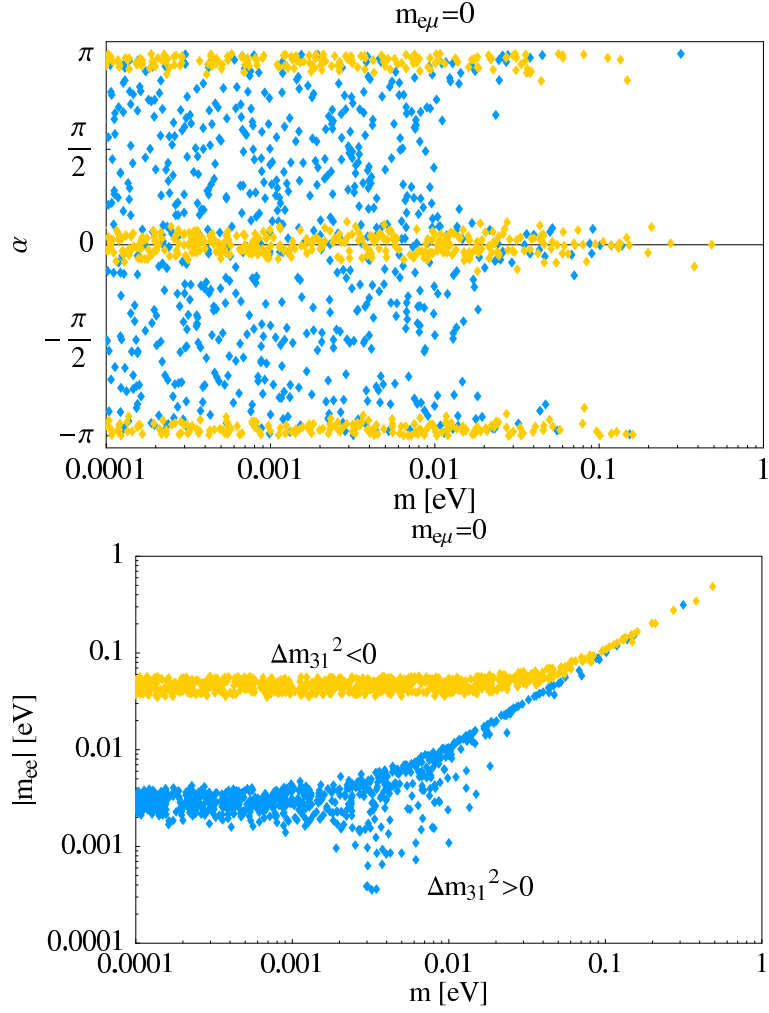


Figure 3: Neutrino observables for  $m_{e\mu} = 0$ . The upper plot is the smallest mass against the Majorana phase  $\alpha$  and the lower plot is the smallest mass against the effective mass. We varied the oscillation parameters within their  $3\sigma$  ranges.

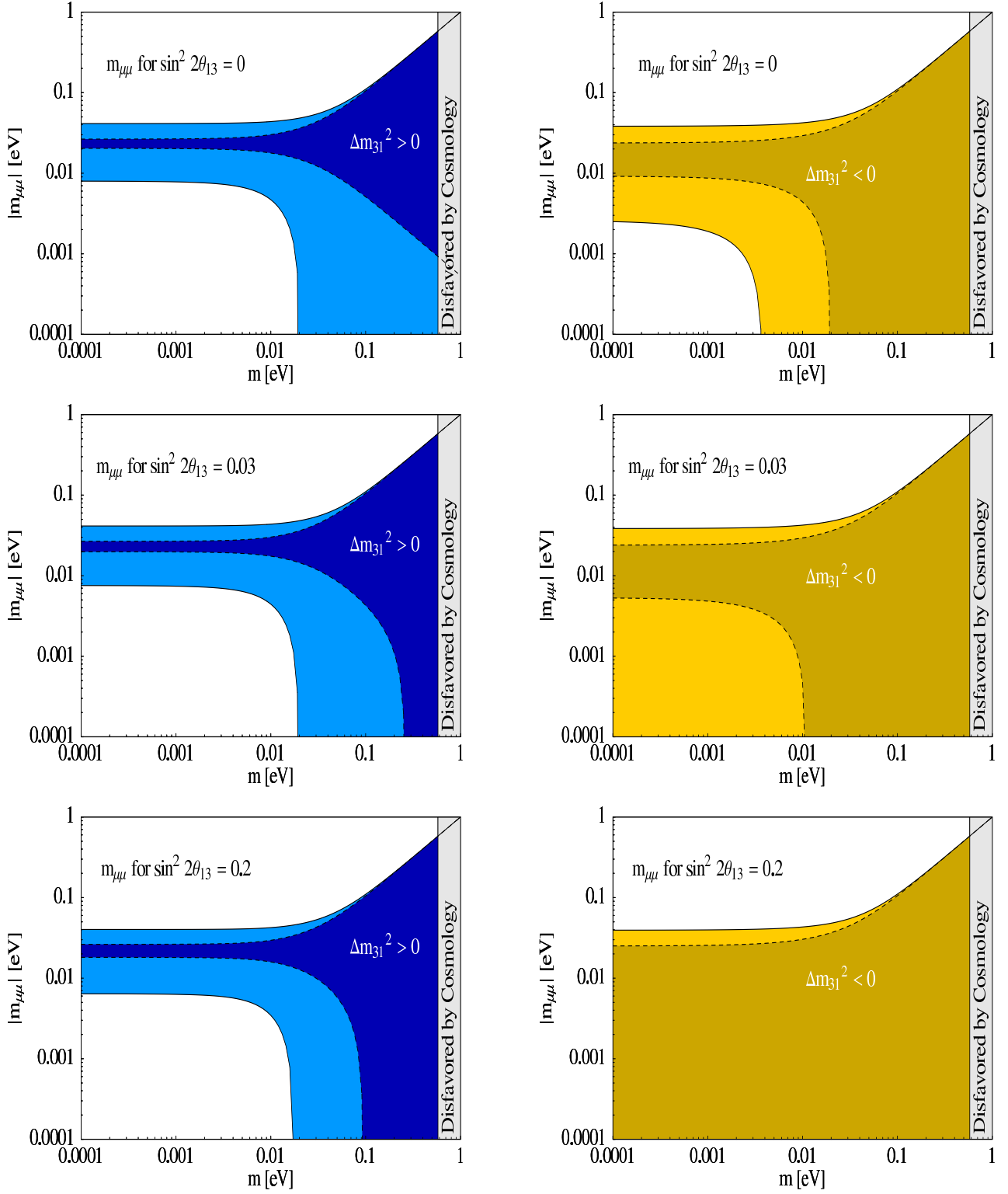


Figure 4: The absolute value of the mass matrix element  $m_{\mu\mu}$  against the smallest neutrino mass for the normal and inverted mass ordering for three representative values of  $\theta_{13}$ . The normal (inverted) mass ordering is given on the left (right) side. The corresponding plot for  $m_{\tau\tau}$  looks basically identical.

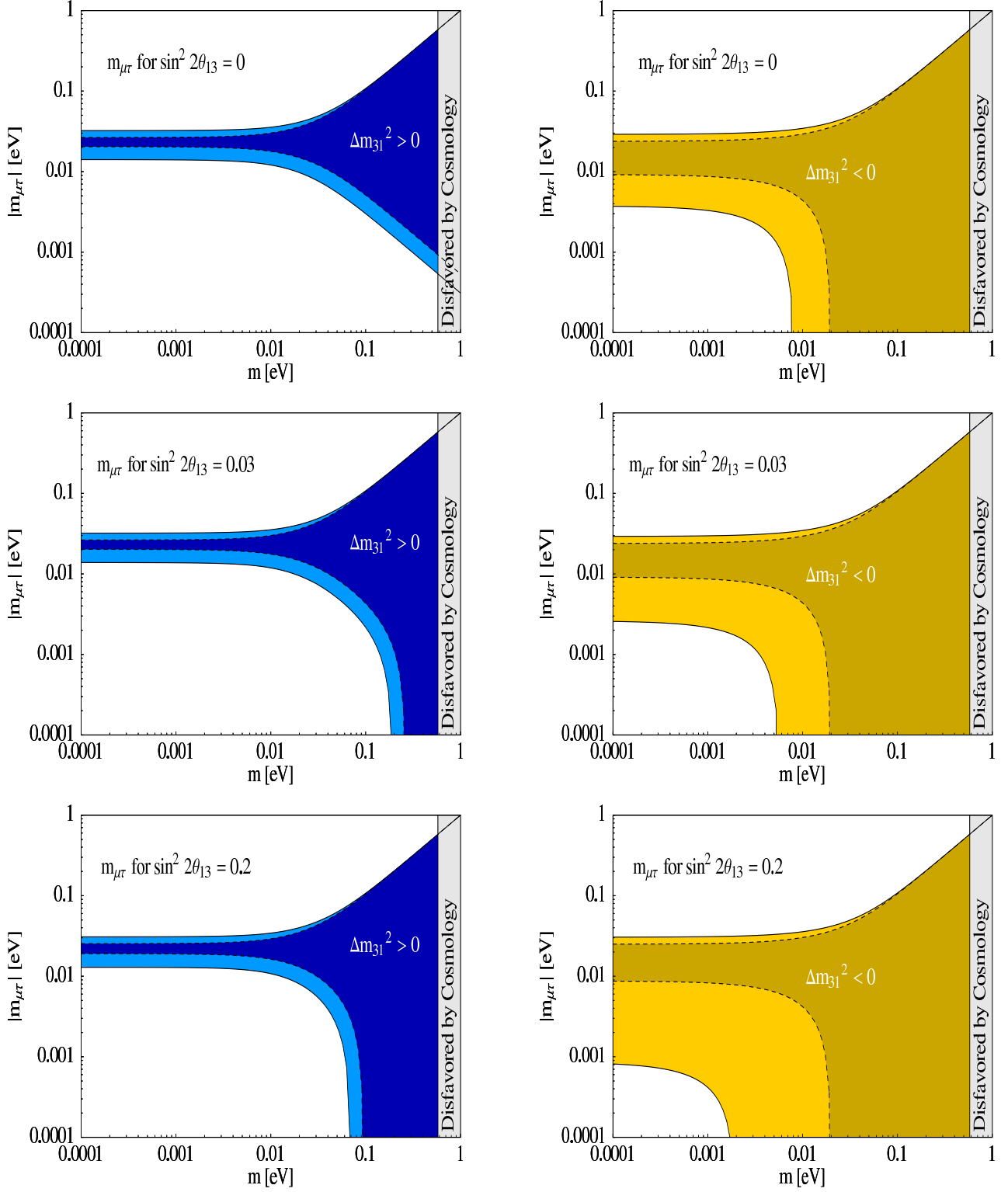


Figure 5: The absolute value of the mass matrix element  $m_{\mu\tau}$  against the smallest neutrino mass for the normal and inverted mass ordering for three representative values of  $\theta_{13}$ . The normal (inverted) mass ordering is given on the left (right) side.

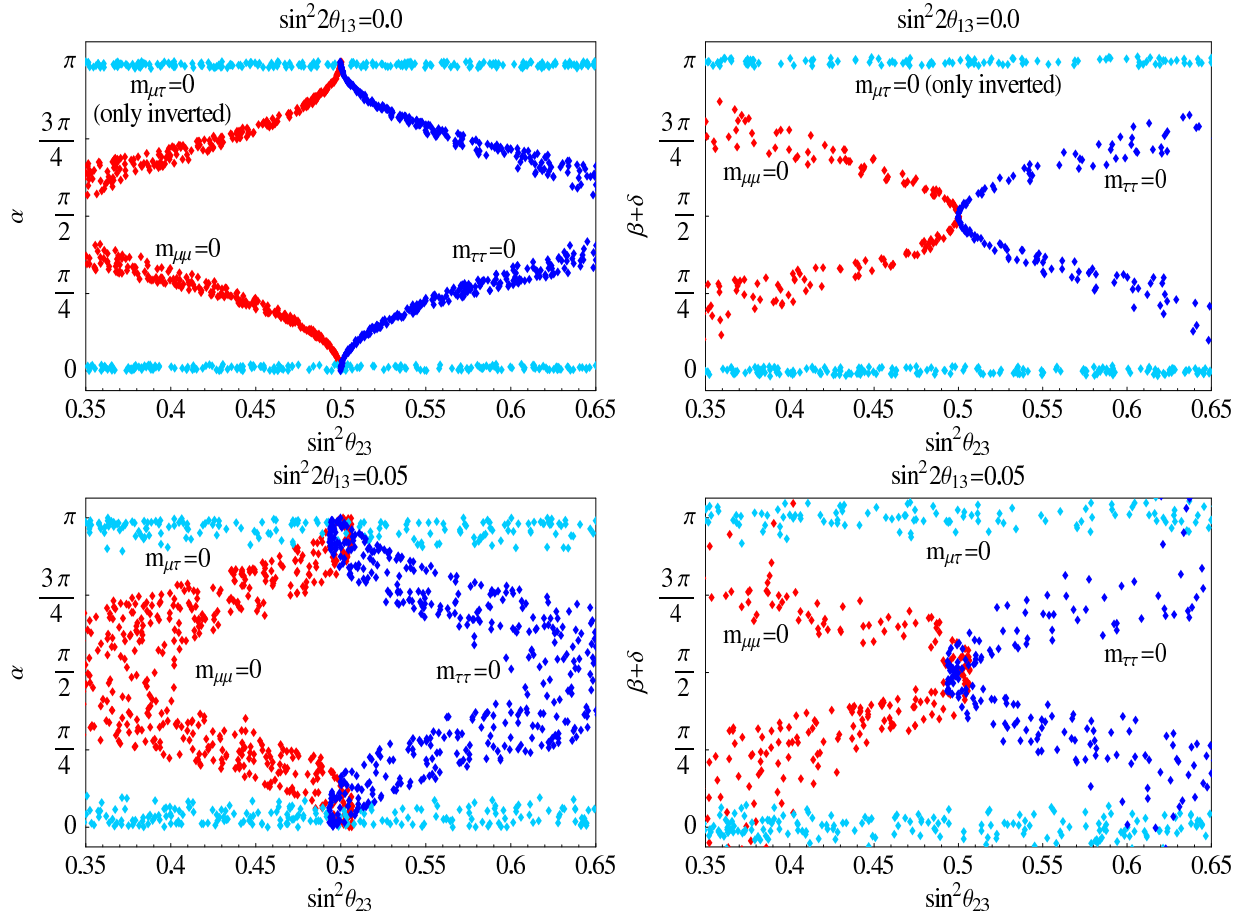


Figure 6: QD neutrinos, vanishing  $\mu\mu$ ,  $\tau\tau$  or  $\mu\tau$  entries and the resulting correlation between  $\theta_{23}$  and  $\alpha$ , and between  $\theta_{23}$  and  $\beta + \delta$ .

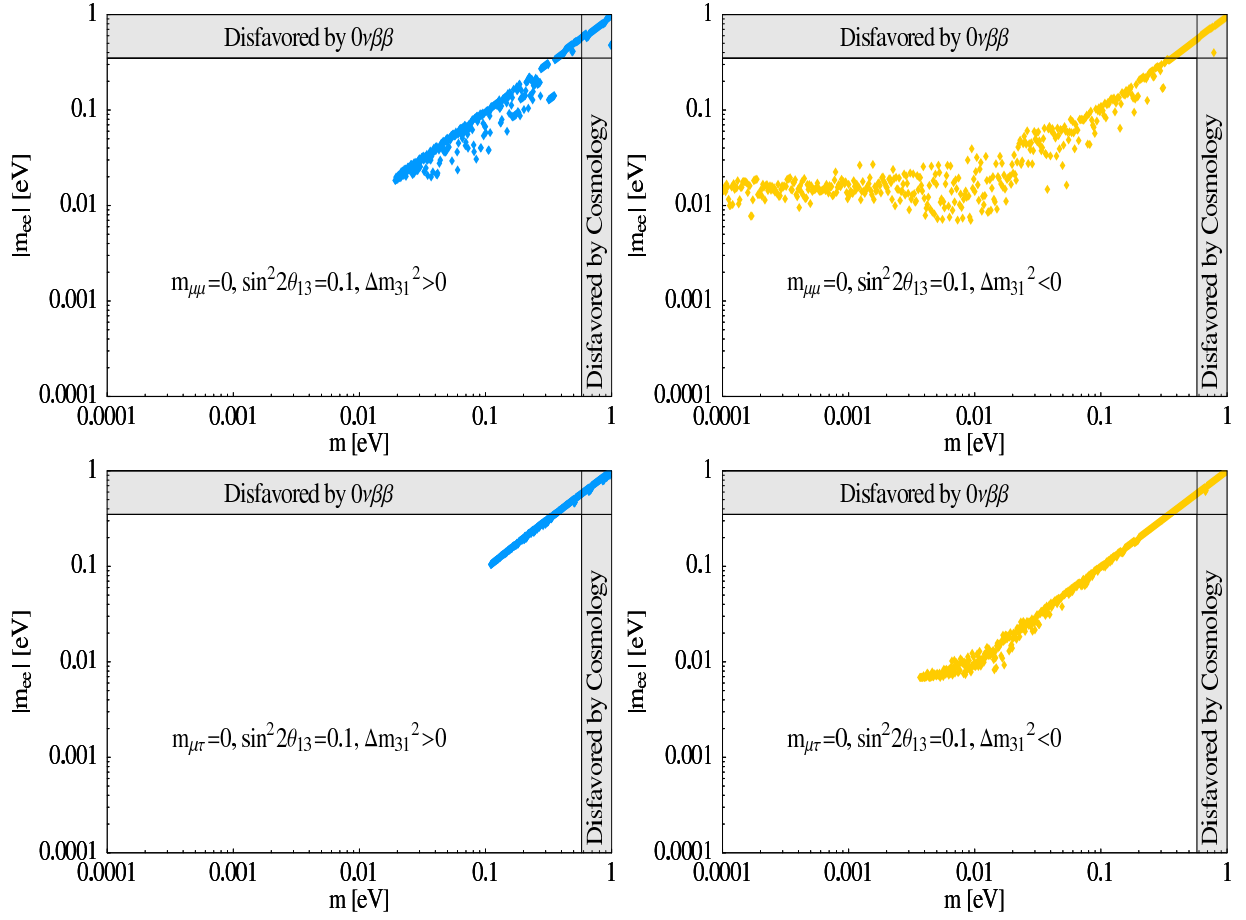


Figure 7: The effective mass  $|m_{ee}|$  in case of  $m_{\mu\mu} = 0$  and  $m_{\mu\tau} = 0$  for  $\sin^2 2\theta_{13} = 0.1$ .